Closed-form approximations of first-passage distributions for a stochastic decision making model

Broderick, T. *et al.* (2009) "Closed-Form Approximations of First-Passage Distributions for a Stochastic Decision-Making Models,"
Applied Mathematics Research eXpress, Vol. 2009, No. 2, pp. 123–141
Advance Access publication February 11, 2010
doi:10.1093/amrx/abp008

Closed-Form Approximations of First-Passage Distributions for a Stochastic Decision-Making Model

Tamara Broderick[1], Kong Fatt Wong-Lin[2,3], and Philip Holmes[2,3,4]

[1]Department of Statistics, University of California, Berkeley, CA 94720, USA, [2]Program in Applied and Computational Mathematics, Princeton University, Princeton, NJ 08544, USA, [3]Neuroscience Institute, Princeton University, Princeton, NJ 08544, USA, and [4]Department of Mechanical and Aerospace Engineering, Princeton University, Princeton, NJ 08544, USA

Correspondence to be sent to: pholmes@math.princeton.edu

In free response choice tasks, decision making is often modeled as a first-passage problem for a stochastic differential equation. In particular, drift-diffusion processes with constant or time-varying drift rates and noise can reproduce behavioral data (accuracy and response-time distributions) and neuronal firing rates. However, no exact solutions are known for the first-passage problem with time-varying data. Recognizing the importance of simple closed-form expressions for modeling and inference, we show that an interrogation or cued-response protocol, appropriately interpreted, can yield approximate first-passage (response time) distributions for a specific class of time-varying processes used to model evidence accumulation. We test these against exact expressions for the constant drift case and compare them with data from a class of sigmoidal functions. We find that both the direct interrogation approximation and an error-minimizing interrogation approximation can capture a variety of distribution shapes and mode numbers but that the direct approximation, in particular, is systematically biased away from the correct free response distribution.

Received July 3, 2009; Revised November 30, 2009; Accepted December 15, 2009

1 Introduction

Stochastic differential equations (SDEs) are widely used to model phenomena in physics and biology in which mixed deterministic and random forces drive a dynamical process. Here, our motivation derives from the neurobiology of decision processes, among the simplest of which is the two-alternative, forced-choice task (2AFC). In each trial of this task, subjects are asked to correctly identify a noisy stimulus drawn at random from two possibilities. In a common instantiation employed on primates and humans, the stimuli are arrays of dots, a fraction of which move coherently either to the left or to the right, while the remainder fluctuate randomly [34, 37]. The difficulty of this motion discrimination task can be manipulated by varying the coherence. Subjects may be either allowed to respond with their perceptual choice in their own time (the *free response protocol*) or required to respond upon presentation of a cue (idealized below as the *interrogation protocol*) [18, 20, 24, 36].

The 2AFC problem has an optimal solution, provided by the sequential probability ratio test (SPRT) [22, 43, 44]. As described in [2], the drift-diffusion model (DDM) is a continuum limit of the SPRT. The DDM SDE classically takes the form

$$dy = \pm A\,dt + \sigma\,dW, \quad y(0) = y_0, \tag{1}$$

where $y(t)$ represents the evolving logarithmic likelihood ratio of the two possibilities, σ is the standard deviation of a Wiener (white noise) process $W(t)$, and A denotes the constant drift rate. In the example above, the stimulus motion direction determines the sign of A, and σ can model noise in the stimulus or within the brain, or both.

In the free response case, Equation (1) is supplemented by two absorbing barriers or thresholds, $y = \pm Z$ with $Z > |y_0|$. First crossing of either by a sample path $y(t)$ signals a response corresponding to that choice: e.g., if $A > 0$ and $+Z$ is crossed first, a correct choice is made; if $-Z$ is crossed first, it is an error. The first-passage time is the decision time (DT). (The behavioral observable is the response or reaction time (RT), which includes the latency of signal transduction and motor preparation, typically modeled as a constant overhead T_0, so that $\mathrm{RT} = \mathrm{DT} + T_0$.)

Under the interrogation protocol, sample paths of Equation (1) are allowed to evolve until a cue time T at which the sign of $y(T)$ determines the response. Again assuming that $A > 0$, the choice is correct if $y(T) > 0$; if $y(T) < 0$ it is an error. This is a continuum version of the Neyman–Pearson fixed sample size decision procedure [27]. Figure 1 illustrates both protocols.

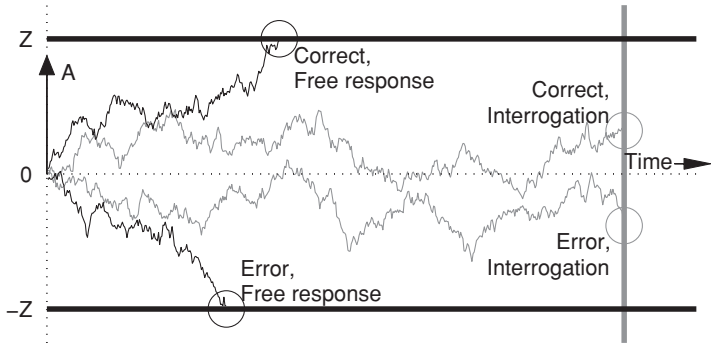

Fig. 1. Illustration of the free response and interrogation protocols for positive drift rate A. *Free response*: The two horizontal black lines are the absorbing thresholds at $\pm Z$; first-passage times of two sample paths (black) are indicated by black circles. *Interrogation*: The vertical gray line is the cue time; locations of two sample paths (gray) at cue time are indicated by gray circles.

In neural models, $y(t)$ is equivalent to the difference in the instantaneous neural activities encoding opposing decisions. Furthermore, Equation (1) can also be derived from more realistic leaky competing accumulator network models of neural function [2–4]. Overall, the DDM not only matches human behavioral data [28, 29, 33, 39] but also qualitatively describes neuronal activities in oculomotor brain areas of monkeys performing the 2AFC tasks. Specifically, short-term firing rates of neurons corresponding to the selected choice rise toward a threshold while those of neurons corresponding to the alternative choice decrease over time [18, 30, 34, 36], such that their difference behaves much like sample drift-diffusion paths.

However, the classical, pure DDM fails to account for certain data. For example, recent studies of the moving dots discrimination task suggest that time-dependent drift rates $A(t)$ provide better matches to behavioral and neuronal data [5, 7–9, 19]. Moreover, in the more complex Eriksen flanker task [10], a subject must decide which of two characters, $<$ or $>$, appears in the center of a stimulus array. In the compatible case, the target character is flanked by copies of itself (e.g. $<<<<<$) and in the incompatible case by copies of the competing stimulus ($>><>>$). Accuracies in these two cases exhibit distinctly different shapes as functions of response time: in the latter, accuracy dips below 50% for low response times before recovering and rising toward 100%, albeit remaining below the monotonically rising accuracy for compatible trials. A neural network model that includes multiple decision units and an attention module that progressively biases the central units accounts for this behavior [6] and can be reduced to a DDM,

also with time-dependent drift [23]. Other models of attention also exhibit time-varying drift rates [40, 41]. This prompts the study of first-passage times for such "extended" DDMs. Other extensions—including drift rates and initial conditions $y(0)$ that are randomized on a trial-by-trial basis [31, 32] and time-varying thresholds [9, 13]—have been considered elsewhere.

The article is organized as follows. In Section 2, we review the pure DDM and explore numerically generated first-passage distributions for a sigmoidal time-dependent drift rate and noise originally proposed to match data from primate experiments [9]. In Section 3, we derive closed-form approximations for first-passage distributions from sample path distributions $p(y,t)$, under the assumption that both drift rate and noise level monotonically approach limits. We compare these predictions with numerical simulations of the free response model with constant and sigmoidal drift rates, and show that, if parameter values are appropriately adjusted, the approximations can be improved. A discussion ensues in Section 4.

2 Effect of Drift Rate and Noise on Response-Time Distributions

We first review classical results for the DDM with constant drift rate. We then introduce a sigmoidal function, similar to that of [9], to describe drift and noise, and explore its implications for correct and error response-time distributions by varying two key parameters.

2.1 Constant drift rate and noise

We begin by assuming both constant drift A and constant noise σ in Equation (1). Without loss of generality, we will assume that $A > 0$ so that the threshold $+Z$ (or $y(T) > 0$ at cue time) corresponds to the correct choice. Also, for simplicity, we will restrict to unbiased initial conditions $y(0) = 0$. Before describing the results, we observe that the SDE (1) can be rescaled by letting $y = Ax$:

$$dx = dt + \left(\frac{\sigma}{A}\right) dW, \quad x(0) = 0, \tag{2}$$

with thresholds $\pm Z/A$. This reduces the three parameters A, σ, and Z to two, the signal-to-noise ratio (SNR), and the threshold-to-drift ratio:

$$\beta = (A/\sigma)^2 \quad \text{and} \quad \alpha = Z/A. \tag{3}$$

First-passage time distributions yielding mean DTs, and error rates (ER) may be computed for (1) from the backward Kolmogorov or Fokker–Planck equation [15, 38]

associated with (2):

$$\langle \mathrm{DT} \rangle = \alpha \tanh(\alpha\beta), \quad \mathrm{ER} = \frac{1}{1+\exp(2\alpha\beta)}, \tag{4}$$

and an explicit expression for the distribution of first-passage times at the threshold $+\alpha$ (or $+Z$) is available [11, 29, 38]:

$$f_+(t) = \frac{\pi}{4\alpha^2\beta} \exp\left[\alpha\beta - \frac{1}{2}\beta t\right] \times \sum_{k=1}^{\infty} k \exp\left[-\frac{k^2\pi^2 t}{8\alpha^2\beta}\right] \sin\left[\frac{k\pi}{2}\right]. \tag{5}$$

For Equation (2) (and (1)), the first-passage distributions for both thresholds $\pm\alpha$ are identical expressions, scaled by the ratio of errors over correct responses:

$$f_-(t) = \left(\frac{\mathrm{ER}}{1-\mathrm{ER}}\right) f_+(t). \tag{6}$$

Notably, correct and error response distributions have identical mean DTs; indeed, both distributions are identical up to a scaling factor and they are unimodal.

2.2 Time-varying drift rate and noise

Having equal-mean correct and error DTs in the DDM is too restrictive for typical experimental data. In some instances, error DTs have been found to be longer than correct DTs [9, 25, 32, 34], particularly when accuracy is emphasized. At other times shorter error DTs have been observed [23, 24, 32], particularly when speed is emphasized. As noted above, variation of initial conditions and drift rates from trial to trial can also produce fast and slow errors, respectively [31].

Seeking a more flexible model, we generalize Equation (1) to an SDE in which drift and noise are time-dependent [38]:

$$dy = A(t)\,dt + \sigma(t)\,dW, \quad y(0) = y_0. \tag{7}$$

We are particularly interested in the sigmoidal function for $A(t)$ and $\sigma(t)$, proposed as Model 4 in [9], that has been shown to fit both behavioral and neuronal data well and can also produce bimodal response-time distributions. Both the drift rate $A(t) = Ag(t)$ and noise $\sigma(t) = \sigma|g(t)|$ are scaled by a sigmoidal *gain function* $g(t)$:

$$g(t) = \frac{1}{G}\left[\frac{1}{1+\exp(-\gamma(t-\delta))} - \eta\right], \tag{8}$$

where G is a normalization constant (see below). Gain is applied to both drift rate and noise since direct neural recordings in primates reveal that these quantities typically wax and wane in concert [16, 17]. Equation (8), which is qualitatively similar to, but

simpler than, the expression of [9], is characterized by the parameters $\gamma \geq 0$, η, and δ, rises monotonically to the limit $(1-\eta)/G$ as $t \to \infty$, and reduces to the constant drift case when $\gamma = 0$.

We wish to study how the parameters that define $g(t)$ affect choice probabilities and DTs; the timescale parameter γ and gain offset η are of particular interest. To make fair comparisons among different cases, we adjust G as follows. We choose a sufficiently late time T such that at least 99% of the probability mass of the normalized first-passage distribution for constant drift and noise falls to the left of $t = T$:

$$0.99 < \int_0^T [f_+(t) + f_-(t)]\, dt < 1, \tag{9}$$

and set G such that the average modulus of the gain over $[0, T]$ is unity:

$$\frac{1}{T}\int_0^T |g(t)|\, dt = 1. \tag{10}$$

G can be obtained as an explicit function of γ, η, and δ $(= 0)$ by using the time at which gain changes sign from negative to positive:

$$t_0 = \delta + \frac{1}{\gamma}\log\left(\frac{\eta}{1-\eta}\right), \tag{11}$$

and the form of the integrated sigmoid:

$$I_g(t) = \int_0^t \frac{ds}{1+\exp(-\gamma(s-\delta))} = t + \frac{1}{\gamma}\log\left[\frac{1+\exp(-\gamma(t-\delta))}{1+\exp(\gamma\delta)}\right]. \tag{12}$$

Specifically, Equation (10) implies that

$$G = \frac{1}{T}[I_g(T) - \eta T - 2(I_g(t_0) - \eta t_0)]. \tag{13}$$

Analytical expressions analogous to those of Equations (4–5) for the constant drift case are unknown for time-varying drifts, so we use the numerical method of [9, Appendix B.4] to investigate the effect of varying the timescale and offset parameters γ and η. Since the DDM is typically assumed to reset at $y(0) = 0$ at each stimulus onset, we take the time offset $\delta = 0$ throughout, and, for simplicity, in the remainder of this section we set the drift and noise scaling factors $A = \sigma = 1$ and thresholds $Z = \pm 1$. Consistent with the assumption $A > 0$ of Section 2.1, we restrict $\eta < 1$ so that the asymptotic value of $Ag(t)$ is strictly positive and crossing of the upper threshold $+Z$ represents a correct decision. Note that $g(t)$ takes negative values for $t > \delta (= 0)$ if and only if $\eta > 0.5$. Representative distributions appear in dark gray in Figure 5 below; the other curves in this figure are described in Section 3.

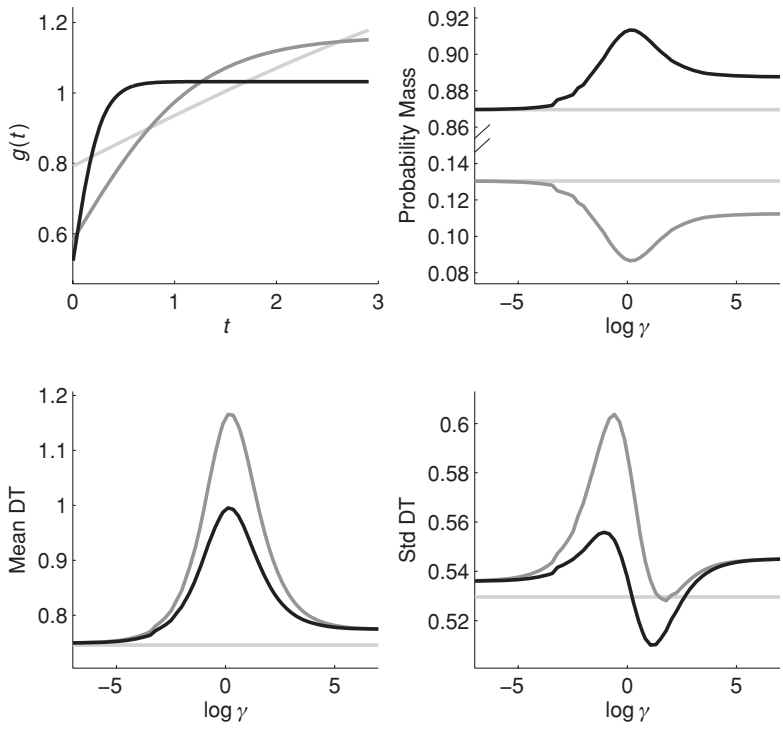

Fig. 2. *Upper left*: Gain functions for $\log\gamma = -1$, 0.5, and 2, with $\delta = \eta = 0$ fixed and $A = \sigma = Z = 1$. Darker colors represent higher values of γ. *Upper right*: First-passage probabilities for upper and lower barriers as a function of γ. In this and the remaining panels, black represents the correct response distribution statistics, dark gray represents the error statistics, and light gray shows the constant gain statistic(s) for comparison. *Lower left*: DT means as a function of γ. *Lower right*: DT standard deviations as a function of γ.

2.3 Timescale parameter γ

In Figure 2 we explore how the timescale γ affects gain and, thereby, the first-passage distributions. We keep the gain offset η fixed at zero. The upper left panel shows three representative gain functions, with darker colors representing higher values of γ. For $\gamma \approx 0$ the normalized gain is almost linear for small t. As γ increases, the sigmoid becomes more pronounced and the maximum gain value decreases due to normalization. Ultimately, as γ becomes very large, gain approaches a constant after an increasingly short transient.

The remaining three panels of Figure 2 illustrate how representative statistics of the resulting first-passage time distributions change with γ, respectively showing

the total probabilities of correct responses and errors (upper right), means (lower left), and standard deviations (lower right). We employ a logarithmic scale to accommodate a wide γ range. The constant drift statistics, which are identical for both correct and error responses, are illustrated for comparison. Differences between correct and error distributions for time-varying gains are particularly striking. The model can clearly account for longer mean error DTs than correct DTs.

2.4 Offset parameter η

Next, we next take a nontrivial timescale, namely, $\gamma = 1$, and vary η to explore how the offset affects the first-passage distributions in the presence of a sigmoidal gain shape. The upper left panel of Figure 3 shows three representative gain functions, with darker shades representing increasing values of η. For η small, gain is entirely positive, but as η increases $g(t)$ changes sign. Such a change may reflect evidence switching directions, perhaps as in the Eriksen flanker task [10, 23]. Note that vertical scales change across η values due to the normalization process described above.

As η increases, gain is increasingly negative at early times and remains so for a longer period, so we expect to see errors become more probable until they are the most likely response. This expectation is borne out in the upper right panel of Figure 3, which shows the total probabilities for correct choices and errors. For comparison, the corresponding probabilities for the constant drift case are also shown.

Perhaps the most interesting feature of the distributions resulting from changes in the sign of sigmoidal drift is the multimodality evident in some of the distributions in Figure 5 (below). Unlike the constant drift case, parameter combinations exist that yield at least two modes in the correct and error distributions. These modes are not necessarily the same for correct and error responses, as evidenced by the differing means and standard deviations in the two lower panels of Figure 3.

3 Free Response Approximation Schemes

We now develop closed-form approximations for first-passage distributions resulting from time-dependent drift $A(t)$ and noise functions $\sigma(t)$ appropriate for modeling sensory integration, such as those introduced in Section 2. To motivate our approach, we note that experiments suggest a common mechanism in both interrogation and free response protocols. Some motion discrimination studies [19, 34] feature a fixed-duration stimulus presentation, followed by a delay period before the interrogation cue. Monkeys do not

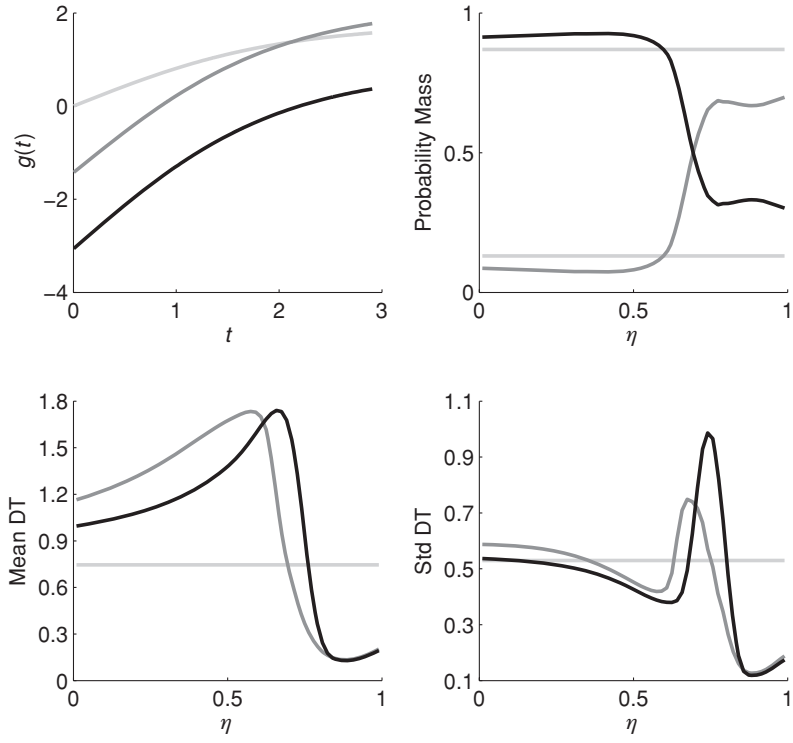

Fig. 3. *Upper left*: Gain functions for $\eta = 0.5$, 0.7, and 0.9, with $\delta = 0$ and $\gamma = 1$ fixed and $A = \sigma = Z = 1$. Darker colors represent higher values of η. *Upper right*: First-passage probabilities for upper and lower barriers as a function of η. In this and the remaining panels, black represents the correct response distribution statistics, dark gray represents the error statistics, and light gray shows the constant gain statistic(s) for comparison. *Lower left*: DT means as a function of η. *Lower right*: DT standard deviations as a function of η.

seem to fully exploit the entire viewing time in these studies; their behavioral choices and neuronal activities being similar under both this and the free response protocol, suggesting that a decision criterion may be reached, and choices "locked in," before response cue (interrogation time).

3.1 Approximation from the interrogation protocol

As noted in Section 1, in the interrogation protocol the first-passage calculation is replaced by simply querying the sign of the sample path $y(T)$ at the interrogation time T. The probability density $p(y, t)$ of finding a solution at y at time t is readily calculated for

the case $y(0) = 0$ by observing that the integral of (7),

$$y(t) = \int_0^t A(s)\,ds + \int_0^t \sigma(s)\,dW_s, \tag{14}$$

is a Gaussian process with mean and variance at t:

$$\mu(t) = \int_0^t A(s)\,ds \quad \text{and} \quad \nu(t) = \int_0^t \sigma^2(s)\,ds, \tag{15}$$

respectively; it therefore follows that

$$p(y,t) = \frac{1}{\sqrt{2\pi\,\nu(t)}} \exp\left[-\frac{(y-\mu(t))^2}{2\nu(t)}\right]. \tag{16}$$

(Equations (15–16) can also be obtained by solving the Fokker–Planck or forward Kolmogorov equation [11, 12, 15], which applies to more general SDEs with x-dependent vector fields.)

Given Equations (15–16), it is straightforward to calculate the rate of change of probability mass through response thresholds at $\pm Z$ with respect to time. For the correct barrier $+Z$, we have

$$\frac{\partial}{\partial t}\mathbb{P}(y > Z, t) = \frac{\partial}{\partial t}\int_{y=Z}^{\infty} p(y,t)\,dy = \frac{1}{\sqrt{2\pi}} \exp\left[-\frac{(Z-\mu(t))^2}{2\nu(t)}\right]\left[\frac{\mu'(t)}{\nu(t)^{1/2}} + \frac{(Z-\mu(t))\nu'(t)}{2\nu(t)^{3/2}}\right], \tag{17}$$

and for the error barrier $-Z$,

$$\begin{aligned}\frac{\partial}{\partial t}\mathbb{P}(y < -Z, t) &= \frac{\partial}{\partial t}\int_{y=-\infty}^{-Z} p(y,t)\,dy \\ &= \frac{1}{\sqrt{2\pi}} \exp\left[-\frac{(Z+\mu(t))^2}{2\nu(t)}\right]\left[-\frac{\mu'(t)}{\nu(t)^{1/2}} + \frac{(Z+\mu(t))\nu'(t)}{2\nu(t)^{3/2}}\right].\end{aligned} \tag{18}$$

This calculation of average probability currents includes sample paths that exit $[-Z, Z]$ prior to time t but subsequently reenter and lie within it at time t. It therefore provides lower bounds for cumulative first-passage distributions, underestimating them in general and offering good approximations only when, after first crossing Z or $-Z$, the subsequent fraction of time spent in $[-Z, Z]$ is small. Finally, we set the approximate first-passage densities equal to Equations (17–18), with (small) adjustments to ensure that they are nowhere negative:

$$\hat{f}_+(t) = \max\left\{0, \frac{\partial}{\partial t}\mathbb{P}(y > Z, t)\right\}, \quad \hat{f}_-(t) = \max\left\{0, \frac{\partial}{\partial t}\mathbb{P}(y < -Z, t)\right\}. \tag{19}$$

Not all processes are amenable to this treatment. For example, a periodic drift rate $A(t) = \sin t$ and decaying noise coefficient $\sigma(t) = e^{-t}$ results in a density $p(y,t)$ with finite variance $\nu(t) \to 0.5$, whose mean drifts back and forth between 0 and 2, repeatedly recrossing $Z = 1$. This leads to a quasiperiodic $\mathbb{P}(y > Z, t)$ and a nonintegrable function

$\hat{f}_+$. (We are indebted to one of the referees for this counterexample.) To ensure that the expressions of Equation (19) are integrable, we assume that both the drift and diffusion coefficients $A(t)$ and $\sigma(t)$ monotonically approach finite limits and that the former is nonzero, so that almost all sample paths leave $[-Z, Z]$ as $t \to \infty$ and $\mathbb{P}(y > Z, t)$ and $\mathbb{P}(y < -Z, t)$ are well-defined distributions. This condition is satisfied for the sigmoidal gain of Section 2.2, which modulates both drift rate and noise and changes sign at most once, and we believe that other biologically relevant sensory integration models would also satisfy it: in particular, persistent reversals in drift are unlikely in 2AFC. (In other tasks, including binocular rivalry, reversals can persist [1].)

For constant gain A and noise variance σ^2, we have $\mu(t) = At$ and $\nu(t) = \sigma^2 t$, and our treatment is similar to the "Wiener diffusion approximation" of [21, Equation (4)]. For the sigmoidal gain $g(t)$ of Equation (8), the functions $\mu'(t) = Ag(t)$ and $\nu'(t) = \sigma^2 g^2(t)$ can be integrated to obtain

$$\mu(t) = \frac{A}{G}[I_g(t) - \eta t] \quad \text{and} \quad \nu(t) = \frac{\sigma^2}{G^2}\left[I_g^{(2)}(t) - 2\eta I_g(t) + \eta^2 t\right], \tag{20}$$

where $I_g(t)$ is given in Equation (12), and the integral of the squared sigmoid is

$$I_g^{(2)}(t) = \int_0^t \left[\frac{1}{1 + \exp(-\gamma(s - \delta))}\right]^2 ds = \left.\frac{-1}{\gamma[1 + \exp(-\gamma(s - \delta))]}\right|_{s=0}^{t} + I_g(t). \tag{21}$$

Thus, in the case of interest, the approximate first-passage distributions are represented entirely in closed form and may be quickly computed using Equations (17–21).

3.2 Evaluation of the interrogation approximation

Having shown that the closed-form distributions provided by the interrogation approximation are convenient, it remains to check that they are acceptably close to the true first-passage distributions. We consider two cases: the "direct" approximation of Section 3.1 with the same parameters as the original diffusion process, and an approximation with parameters chosen to minimize the sum-of-squares error (SSE) distance between the interrogation approximation and the (simulated) free response model. As expected, the SSE-minimizing distributions can better match the simulated free response distributions, at the cost of defining different effective drift and threshold values.

To minimize SSE, we use both the default unconstrained nonlinear optimization algorithm `fminsearch` in Matlab, and simulated annealing (code available from `http://www.mathworks.com/matlabcentral/fileexchange/10548`.), taking parameter values from the method that produces the smallest SSE. In the constant-gain case, we

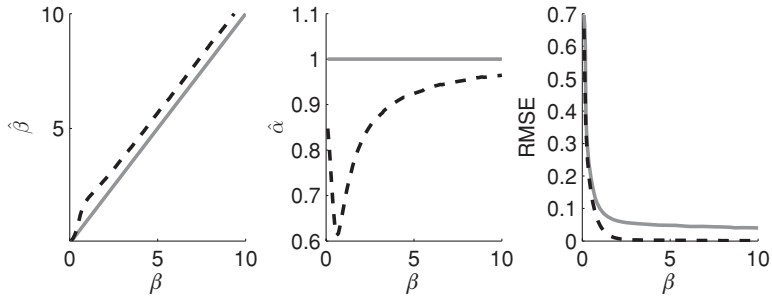

Fig. 4. SSE-minimizing parameters of the interrogation approximation to free response first-passage distributions are displayed for different signal-to-noise ratios (SNRs) β and fixed threshold-to-drift ratio α. *Left*: Dashed line shows SSE-minimizing SNR $\hat{\beta}$; true β is shown as solid line (of unit slope). *Center*: Dashed line shows SSE-minimizing threshold-to-drift ratio $\hat{\alpha}$; true $\alpha(=1)$ is shown as solid line. *Right*: Dashed line shows root mean squared error (RMSE) of the approximation using the SSE-minimizing parameters; solid line shows RMSE for the actual parameters.

allow Z, A, and σ^2 to vary in our minimization, expressing the results in terms of the SNR $\beta = (A/\sigma)^2$ and threshold-to-drift ratio $\alpha = Z/A$ defined in Section 2.1. In the time-varying case, we further allow the gain parameters γ, δ, and η to vary, and, working with A/G and σ^2/G^2, we use Equation (20) to bypass explicit calculation of the normalization constant G. For both constant and time-varying gains, parameters were kept constant across the upper and lower threshold distributions. SSE was calculated as a sum of the SSEs at each threshold, with SSEs weighted equally at both thresholds.

3.2.1 *Constant gains*

It was noted in [21] that, for certain distributions in the constant gain case, the SSE-minimizing parameters differ from the original free response parameters. In Figure 4, we explore this discrepancy systematically as a function of SNR β. The left panel compares the true β with the SSE-minimizing value $\hat{\beta}$ as β varies with constant threshold-to-drift ratio α. The middle panel compares the true (constant) α with the SSE-minimizing $\hat{\alpha}$-value across the same set of models. Systematic differences between the generating and best-fit parameters are evident. For $\beta > 2$ a simple translation $\hat{\beta} \approx \beta + 0.7$ suffices to predict $\hat{\beta}$. The α case is more complex, but $\hat{\alpha} < \alpha$ and $\hat{\alpha}$ approaches α from below as β increases.

This finding is consistent with the fact that the interrogation approximation underestimates the fractions of sample paths that have first exited the barriers $\pm Z$

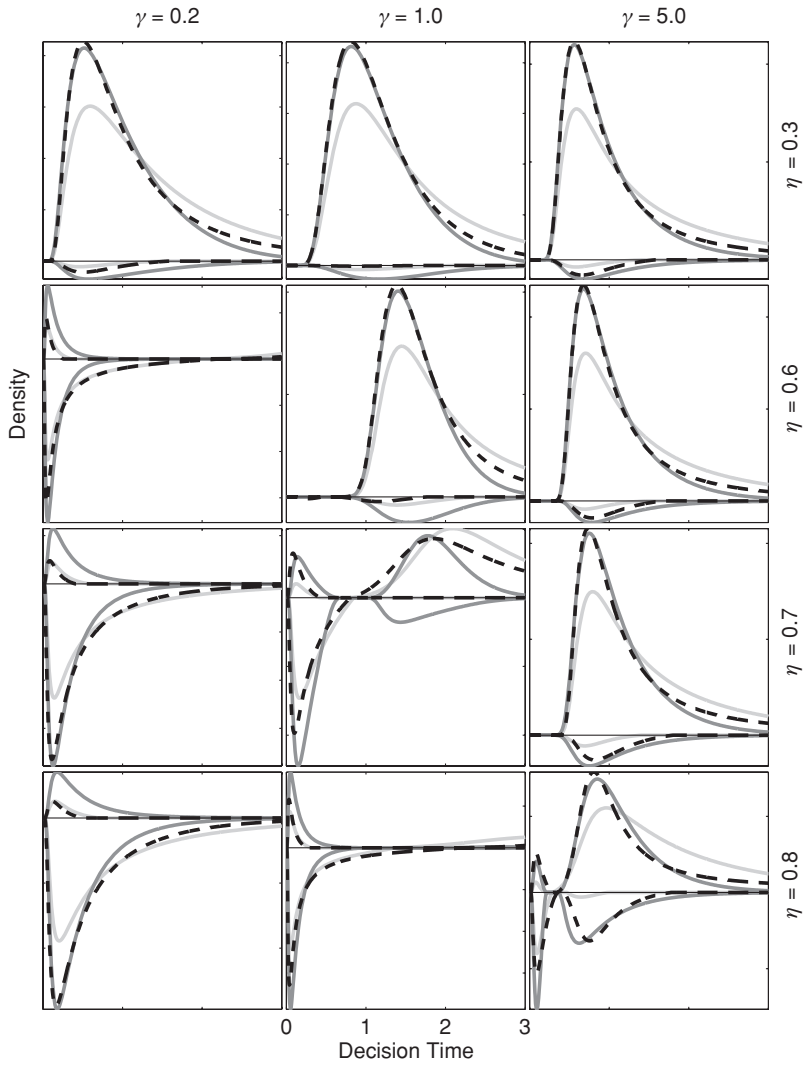

Fig. 5. A diverse set of free response distributions generated by time-varying sigmoidal gains with $\delta = 0$ (dark gray). Also shown are the direct interrogation approximations (light gray) and the SSE-minimizing interrogation approximations (dashed black). Upper and lower curves in each square are correct and error DT distributions, respectively. To better compare approximations, distributions are not normalized and different vertical scales are used in each panel.

at time t. Thus, the true first-passage distribution is underestimated at shorter times and overestimated at longer times (see Figure 5). This discrepancy is partially repaired by *increasing* the effective SNR $\hat{\beta}$, thereby reducing the probability of paths reentering $[-Z, Z]$. A similar effect is achieved by *reducing* the threshold-to-drift ratio $\hat{\alpha}$. Not only is

$\hat{\beta} > \beta$ and $\hat{\alpha} < \alpha$ for all β, but errors for both the original and SSE-minimizing parameters decrease monotonically as β increases (right panel of Figure 4).

This discrepancy has immediate implications for analysis with this model; parameters inferred from, e.g., a Bayesian analysis using the interrogation approximation may be quite far from the true generating parameters at low SNR. Nonetheless, as expected, both the direct and SSE-minimizing approximations approach the true free response distribution at high SNR (right panel of Figure 4), although the latter approaches zero error substantially faster.

3.2.2 *Sigmoidal time-varying gains*

Using the gains of Equation (8), we find a much wider variety of first-passage distributions, as shown in the numerically generated results of Figure 5 (dark gray). Distributions can be unimodal (e.g., $\gamma = 1$, $\eta = 0.3$) or bimodal (e.g., $\gamma = 1$, $\eta = 0.7$); bimodality occurs when $\eta > 0.5$ and gain $g(t)$ changes sign in $[0, T]$, but may not be apparent if this occurs when a few paths have crossed threshold (e.g., $\gamma = 1$, $\eta = 0.6$). While some distributions have greater probability mass at the upper barrier (e.g., $\gamma = 5$, $\eta = 0.6$, where the sign change is very early), others have greater mass at the lower barrier (e.g., $\gamma = 0.2$, $\eta = 0.8$, where the sign change is very late). Some upper and lower distribution pairs are approximately proportional (cf. Equation (6)), but others are noticeably not (e.g., $\gamma = 1$, $\eta = 0.7$). Despite the variety of functional forms and the fact that $g(t)$ changes sign after stimulus onset for $\eta > 0.5$, promoting barrier recrossing (lower three rows), the direct interrogation approximation (19) (light gray) successfully captures the numbers and relative sizes of modes. Also, consistent with its lower bound of cumulative distributions (Section 3.1), it underestimates early peaks and overestimates tails of the true distributions $f_{\pm}$, as the top row of Figure 5 clearly illustrates.

As expected, the SSE-minimizing interrogation approximation (dashed black) also captures mode number and relative sizes, often being very close to the true distributions (e.g., $\gamma = 5, \eta = 0.6$), although sometimes it improves only slightly upon the direct approximation (e.g., $\gamma = 1$, $\eta = 0.8$). However, both approximations sometimes fail to reproduce distributions with low probability mass. We believe that this is due in part to the high probability of boundary recrossing in such cases. The poor SSE-minimizing fits, in particular, are dominated by a larger probability mass crossing the other boundary (e.g., lower barrier for $\gamma = 1$, $\eta = 0.3, 0.6$; upper barrier for $\gamma = 0.2$, $\eta = 0.7, 0.8$).

To provide a more systematic understanding of the approximation's accuracy, in Figure 6 we plot errors for the direct and SSE-minimizing approximations over the

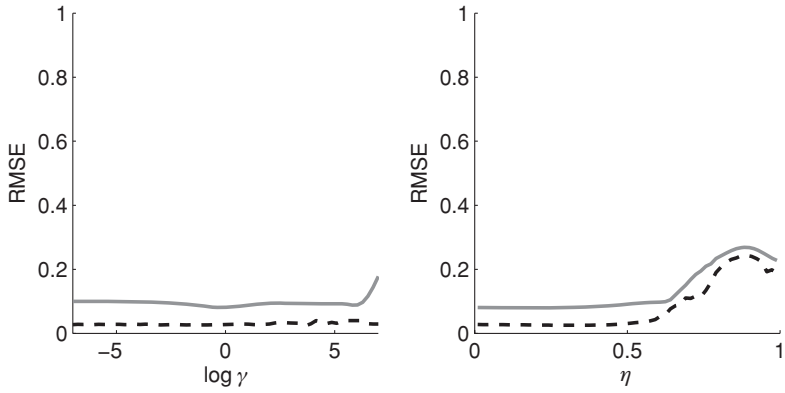

Fig. 6. Root mean squared errors (RMSEs) for interrogation approximations to first-passage distributions calculated across generating γ and η values for the time-dependent DDM with $\delta = 0$, $A = 1$, $\sigma = 1$, and $Z = 1$. Dashed curves show RMSEs for approximations using SSE-minimizing parameters; solid curves show RMSEs for the true parameters. *Left*: RMSEs as a function of γ with $\eta = 0$. *Right*: RMSEs as a function of η with $\gamma = 1$.

parameter ranges used in Section 2 (Figures 2 and 3). At each γ value in the left panel, we define $g(t)$ with the given γ and all other parameters constant, calculate the first-passage distribution numerically [9], and find the direct and SSE-minimizing approximations. Similarly, η is varied in the right panel, with all other gain parameters held constant. This reveals that certain distributions in Figure 5 are among the most problematic to approximate. In particular, the two lower panels of the middle column ($\eta = 0.7, 0.8$) fall in the high-error region of Figure 6 (right panel).

Both approximations compare favorably with the constant gain cases in the right panel of Figure 4 over the remaining parameter values. The direct approximation performs similarly for both constant and time-varying gains. The SSE-minimizing approximation does not do as well for time-varying gain, but it still exhibits lower errors in all cases shown here.

4 Conclusion

In the first part of this article, we investigate first-passage distributions for a drift-diffusion process with time-varying drift rate and noise, as used in modeling human and primate decision making. Confirming earlier work of [9], we show that such a process can generate slower errors, unlike the pure DDM with constant drift and noise, and

we systematically explore the parameter space of a class of sigmoidal gain functions, characteristic of those fitted to behavioral data [9, 34] (Figures 2 and 3).

Time-dependent drift is problematic in that no explicit functions describing first-passage distributions are known, so in the second part we derive such a closed-form expression from a simpler interrogation protocol. For constant drift and noise, this approximation is especially good for high SNRs, in agreement with intuition (Figure 4). As SNR increases, a smaller fraction of sample paths recrosses each decision threshold substantially after the first passage, so that interrogation as to whether the state lies outside the thresholds at time t is a good indicator of first-passage status.

Our approximation is similar in form to that of [21] in the constant drift and noise case, but here we explicitly describe its derivation and systematically evaluate its accuracy. We show that it can capture a variety of distributional shapes exhibited by diffusion processes with time-varying drift and noise modulated by a sigmoidal function that changes sign at most once. Improved approximations may be obtained by optimizing the model parameters to minimize the SSE with numerically simulated first-passage distribution (Figures 4 and 6): a procedure that further illuminates the source of errors in the direct interrogation approximation and highlights possible biases in using closed-form approximations for applications in Bayesian modeling and behavioral analyses.

Under appropriate experimental conditions, subjects can produce errors that are either slower or faster than mean times for correct responses. Models with an intrinsic acceleration toward a decision threshold, e.g., unstable Ornstein–Uhlenbeck process with linear [2, 26, 38, 42] or nonlinear [35, 45] dependence on y, can reproduce slow errors without incorporating time variation. However, their decision thresholds must be significantly changed, or initial conditions chosen asymmetrically, to produce fast errors. In contrast, we show that simply increasing the offset η in the time-varying gain can change slow errors to fast errors. This may be useful in modeling tasks in which cognitive control arrives relatively late in the decision process. Prior biases can be a major cause of errors in such cases (e.g., in the Eriksen task [6, 23]). More generally, modulation of weights among current and recent evidence and prior expectations underlies many decisions [12, 14], and models and methods that can accommodate time-varying evidence streams are therefore likely to be in demand.

In summary, the present closed-form approximation should be valuable not only in approximating various model behaviors in free response choice tasks, but for other first-passage processes with similar time-varying data.

Acknowledgments

This work was supported by PHS grant MH62196 (Cognitive and Neural Mechanisms of Conflict and Control, Silvio M. Conte Center). TB's research was funded by a Marshall Scholarship. We thank Erhan Çinlar for helpful advice, and an anonymous referee for valuable comments, including the counterexample of Section 2.2. Free response model data were generated using the Stochastic Integration Modeling Toolbox [9], generously provided online at `http://www.shadlen.org/~jd/software`.

References

[1] Blake, R., and N. K. Logothetis. "Visual competition." *Nature Reviews Neuroscience* 3 (2002): 13–21.

[2] Bogacz, R., E. Brown, J. Moehlis, P. Holmes, and J. D. Cohen. "The physics of optimal decision making: A formal analysis of models of performance in two alternative forced choice tasks." *Psychological Review* 113, no. 4 (2006): 700–65.

[3] Brown, E., J. Gao, P. Holmes, R. Bogacz, M. Gilzenrat, and J. D. Cohen. "Simple networks that optimize decisions." *International Journal of Bifurcation and Chaos* 15, no. 3 (2005): 803–26.

[4] Brown, E., and P. Holmes. "Modeling a simple choice task: Stochastic dynamics of mutually inhibitory neural groups." *Stochastics and Dynamics* 1 (2001): 159–91.

[5] Churchland, A. K., R. Kiani, and M. N. Shadlen. "Decision-making with multiple alternatives." *Nature Neuroscience* 11 (2008): 693–702.

[6] Cohen, J. D., D. Servan-Schreiber, and J. L. McClelland. "A parallel distributed processing approach to automaticity." *American Journal of Psychology* 105 (1992): 239–69.

[7] Ditterich, J. "Computational Approaches to Visual Decision Making." In *Percept, Decision, Action: Bridging the Gaps*, edited by D. J. Chadwick, M. Diamond, and J. Goode, 114–26. Novartis Foundation Symposium 270. Chichester, UK: Wiley, 2006.

[8] Ditterich, J. "Evidence for time-variant decision making." *European Journal of Neuroscience* 24 (2006): 3628–41.

[9] Ditterich, J. "Stochastic models of decisions about motion direction: Behavior and physiology." *Neural Networks* 19 (2006): 981–1012.

[10] Eriksen, B. A., and C. W. Eriksen. "Effects of noise letters upon the identification of target letters in a non-search task." *Perception and Psychophysics* 16 (1974): 143–49.

[11] Feller, W. *An Introduction to Probability Theory and Its Applications*, 2nd ed. New York: Wiley, 1957.

[12] Feng, S., P. Holmes, A. Rorie, and W. T. Newsome. "Can monkeys choose optimally when faced with noisy stimuli and unequal rewards?" *PLoS Computational Biology* 5, no. 2 (2009): e1000284.

[13] Frazier, P. I., and A. J. Yu. "Sequential Hypothesis Testing under Stochastic Deadlines." In *Advances in Neural Information Processing Systems* 20, edited by J. C. Platt, D. Koller, Y. Singer, and S. Roweis, 465–72. Cambridge, MA: MIT Press, 2008.

[14] Gao, J., K. F. Wong-Lin, P. Holmes, P. Simen, and J. D. Cohen. "Sequential effects in two-choice reaction time tasks: Decomposition and synthesis of mechanisms." *Neural Computation* 21, no. 9 (2009): 2407–36.

[15] Gardiner, C. W. *Handbook of Stochastic Methods,* 2nd ed. New York: Springer, 1985.

[16] Gold, J. I., and M. N. Shadlen. "Representation of a perceptual decision in developing oculomotor commands." *Nature* 404 (2000): 390–94.

[17] Gold, J. I., and M. N. Shadlen. "The influence of behavioral context on the representation of a perceptual decision in developing oculomotor commands." *J. Neurosci* 23 no. 2 (2003): 632–651.

[18] Gold, J. I., and M. N. Shadlen. "The neural basis of decision making." *Annu. Rev. Neurosci* 30 (2007): 535–574.

[19] Kiani, R., T. D. Hanks, and M. N. Shadlen. "Bounded integration in parietal cortex underlies decisions even when viewing duration is dictated by the environment." *Journal of Neuroscience* 28 (2008): 3017–29.

[20] Laming, D. R. J. *Information Theory of Choice-Reaction Times*. New York: Academic Press, 1968.

[21] Lee, M. D., I. G. Fuss, and D. J. Navarro. "A Bayesian Approach to Diffusion Models of Decision-Making and Response Time." In *Advances in Neural Information Processing Systems*, edited by B. Scholkopf, J. C. Platt, and T. Hoffman, 809–15. Cambridge, MA: MIT Press, 2007.

[22] Lehmann, E. L. *Testing Statistical Hypotheses*. New York: John Wiley & Sons, 1959.

[23] Liu, Y., P. Holmes, and J. D. Cohen. "A neural network model of the Eriksen task: Reduction, analysis, and data fitting." *Neural Computation* 20, no. 2 (2008): 345–73.

[24] Luce, R. D. *Response Times: Their Role in Inferring Elementary Mental Organization*. New York: Oxford University Press, 1986.

[25] Mazurek, M. E., J. D. Roitman, J. Ditterich, and M. N. Shadlen. "A role for neural integrators in perceptual decision making." *Cerebral Cortex* 13, no. 11 (2003): 891–98.

[26] Moehlis, J., E. Brown, R. Bogacz, P. Holmes, and J. D. Cohen. "Optimizing Reward Rate in Two Alternative Choice Tasks: Mathematical Formalism." In *Princeton Technical Report #04-01, Center for the Study of Brain, Mind and Behavior* 2004.

[27] Neyman, J., and E. S. Pearson. "On the problem of the most efficient tests of statistical hypotheses." *Philosophical Transactions of the Royal Society, London, Series A* 231 (1933): 289–337.

[28] Palmer, J., A. C. Huk, and M. N. Shadlen. "The effect of stimulus strength on the speed and accuracy of a perceptual decision." *Journal of Vision* 5 (2005): 376–404.

[29] Ratcliff, R. "A theory of memory retrieval." *Psychological Review* 85 (1978): 59–108.

[30] Ratcliff, R., A. Cherian, and M. A. Segraves. "A comparison of macaque behavior and superior colliculus neuronal activity to predictions from models of two choice decisions." *Journal of Neurophysiology* 90 (2003): 1392–1407.

[31] Ratcliff, R., and G. McKoon. "The diffusion decision model: Theory and data for two-choice decision tasks." *Neural Computation* 20, no. 4 (2008): 873–922.

[32] Ratcliff, R., and J. N. Rouder. "Modeling response times for two-choice decisions." *Psychological Science* 9 (1998): 347–56.

[33] Ratcliff, R., T. Van Zandt, and G. McKoon. "Connectionist and diffusion models of reaction time." *Psychological Review* 106, no. 2 (1999): 261–300.

[34] Roitman, J. D., and M. N. Shadlen. "Response of neurons in the lateral interparietal area during a combined visual discrimination reaction time task." *Journal of Neuroscience* 22, no. 21 (2002): 9475–89.

[35] Roxin, A., and A. Ledberg. "Neurobiological models of two-choice decision making can be reduced to a one-dimensional nonlinear diffusion equation." *PLoS Computational Biology* 4 (2008): e1000046.

[36] Schall, J. D. "Neural basis of deciding, choosing and acting." *Nature Reviews Neuroscience* 2 (2001): 33–42.

[37] Shadlen, M. N., and W. T. Newsome. "Neural basis of a perceptual decision in the parietal cortex (area LIP) of the rhesus monkey." *Journal of Neurophysiology* 86 (2001): 1916–36.

[38] Smith, P. L. "Stochastic dynamic models of response time and accuracy: A foundational primer." *Journal of Mathematical Psychology* 44 (2000): 408–63.

[39] Smith, P. L., and R. Ratcliff. "Psychology and neurobiology of simple decisions." *Trends in Neurosciences* 27, no. 3 (2004): 161–68.

[40] Smith, P. L., and R. Ratcliff. "An integrated theory of attention and decision making in visual signal detection." *Psychological Review* 116 (2009): 283–317.

[41] Smith, P. L., R. Ratcliff, and B. J. Wolfgang. "Attention orienting and the time course of perceptual decisions: Response time distributions with masked and unmasked displays." *Vision Research* 44 (2004): 1297–1320.

[42] Usher, M., and J. L. McClelland. "On the time course of perceptual choice: The leaky competing accumulator model." *Psychological Review* 108 (2001): 550–92.

[43] Wald, A. *Sequential Analysis*. New York: John Wiley, 1947.

[44] Wald, A., and J. Wolfowitz. "Optimum character of the sequential probability ratio test." *Annals of Mathematical Statistics* 19 (1948): 326–39.

[45] Wong, K. F., and X. J. Wang. "A recurrent network mechanism of time integration in perceptual decisions." *Journal of Neuroscience* 26, no. 4 (2006): 1314–28.